Single top with FCNC @ CEPC

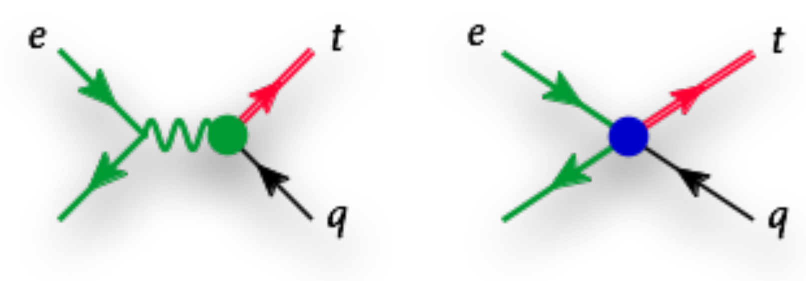

Cen Zhang

Institute of High Energy Physics

CEPC Snowmass EF03 meeting
July 13 2020

Based on 1906.04573 with Liaoshan Shi
and ongoing FCPPL project with Gauthier Durieux, Stefano Frixione, Benjamin Fuks, Hua-Sheng Shao, Liaoshan Shi, Marco Zaro, Xiaoran Zhao

Top FCNC

- Neutral couplings that involve one top quark and one light quark.

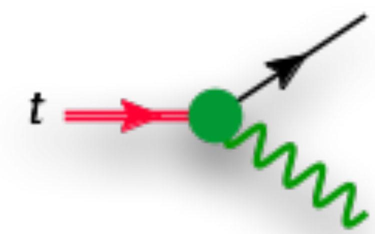

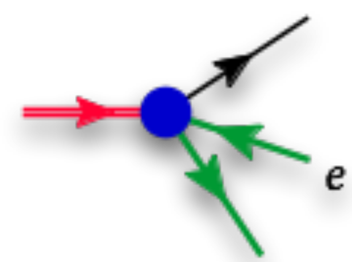

- Forbidden in the SM (by GIM mechanism)
Definite sign of BSM.

	Br^{SM}	Br^{exp}
$t \to cg$	$\sim 10^{-11}$	$\lesssim 10^{-4*}$
$t \to c\gamma$	$\sim 10^{-12}$	$\lesssim 10^{-3*}$
$t \to cZ$	$\sim 10^{-13}$	$\lesssim 10^{-4}$
$t \to ch$	$\sim 10^{-14}$	$\lesssim 10^{-3}$

	SM	QS	2HDM	FC 2HDM	MSSM	$\not{R}$ SUSY
$t \to uZ$	8×10^{-17}	1.1×10^{-4}	–	–	2×10^{-6}	3×10^{-5}
$t \to u\gamma$	3.7×10^{-16}	7.5×10^{-9}	–	–	2×10^{-6}	1×10^{-6}
$t \to ug$	3.7×10^{-14}	1.5×10^{-7}	–	–	8×10^{-5}	2×10^{-4}
$t \to uH$	2×10^{-17}	4.1×10^{-5}	5.5×10^{-6}	–	10^{-5}	$\sim 10^{-6}$
$t \to cZ$	1×10^{-14}	1.1×10^{-4}	$\sim 10^{-7}$	$\sim 10^{-10}$	2×10^{-6}	3×10^{-5}
$t \to c\gamma$	4.6×10^{-14}	7.5×10^{-9}	$\sim 10^{-6}$	$\sim 10^{-9}$	2×10^{-6}	1×10^{-6}
$t \to cg$	4.6×10^{-12}	1.5×10^{-7}	$\sim 10^{-4}$	$\sim 10^{-8}$	8×10^{-5}	2×10^{-4}
$t \to cH$	3×10^{-15}	4.1×10^{-5}	1.5×10^{-3}	$\sim 10^{-5}$	10^{-5}	$\sim 10^{-6}$

Top FCNC

- Neutral couplings that involve one top quark and one light quark.

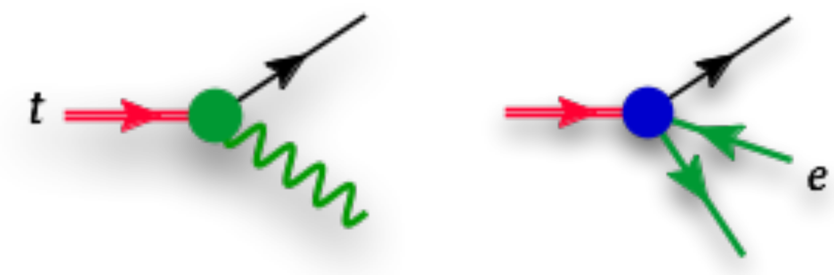

- Forbidden in the SM (by GIM mechanism) **Definite sign of BSM**.

	$\mathrm{Br}^{\mathrm{SM}}$	$\mathrm{Br}^{\mathrm{exp}}$
$t \to cg$	$\sim 10^{-11}$	$\lesssim 10^{-4*}$
$t \to c\gamma$	$\sim 10^{-12}$	$\lesssim 10^{-3*}$
$t \to cZ$	$\sim 10^{-13}$	$\lesssim 10^{-4}$
$t \to ch$	$\sim 10^{-14}$	$\lesssim 10^{-3}$

- A complete and systematic description of FCNC interactions based on **Standard Model Effective Field Theory**:

$$\mathcal{L}_{\mathrm{EFT}} = \mathcal{L}_{\mathrm{SM}} + \sum_i \frac{f_i^{(6)} O_i^{(6)}}{\Lambda^2} + \sum_i \frac{f_i^{(8)} O_i^{(8)}}{\Lambda^4} + \cdots$$

Leading dim-6 FCNC operators are classified in the TOP WG EFT notes.

[Aguilar-Saavedra et al. '18]

Top FCNC: current limits

Mode	$\mathrm{Br}^{95\%\mathrm{CL}}$	Ref.	exp.	$\sqrt{s}$	$\mathcal{L}$	remarks
$t \to qZ$						
u	$\mathbf{1.7 \times 10^{-4}}$	[1176]	ATLAS	13 TeV	$36.1\,\mathrm{fb}^{-1}$	decay, $\lvert m_{\ell\ell} - m_Z \rvert < 15$ GeV
c	$\mathbf{2.4 \times 10^{-4}}$					
u	2.4×10^{-4}	[1177]	CMS	13 TeV	$35.9\,\mathrm{fb}^{-1}$	production plus decay
c	4.5×10^{-4}					
u	2.2×10^{-4}	[1178]	CMS	8 TeV	$19.7\,\mathrm{fb}^{-1}$	production, $76 < m_{\ell\ell} < 106$ GeV
c	4.9×10^{-4}					
$t \to qg$						
u	0.40×10^{-4}	[1179]	ATLAS	8 TeV	$20.3\,\mathrm{fb}^{-1}$	$\sigma(pp \to t) \times \mathrm{Br}(t \to bW) < 3.4$ pb
c	$\mathbf{2.0 \times 10^{-4}}$					
u	$\mathbf{0.20 \times 10^{-4}}$	[1180]	CMS	7, 8 TeV	$5.0, 17.9\,\mathrm{fb}^{-1}$	in $pp \to tj$
c	4.1×10^{-4}					
$t \to q\gamma$						
u	$\mathbf{1.3 \times 10^{-4}}$	[1175]	CMS	8 TeV	$19.8\,\mathrm{fb}^{-1}$	$\sigma(pp \to t\gamma) \times \mathrm{Br}(t \to bl\nu) < 26$ fb
c	$\mathbf{17 \times 10^{-4}}$					$\sigma(pp \to t\gamma) \times \mathrm{Br}(t \to bl\nu) < 37$ fb
$t \to qh$						
u	$\mathbf{19 \times 10^{-4}}$	[1181]	ATLAS	13 TeV	$36.1\,\mathrm{fb}^{-1}$	multilepton channel
c	$\mathbf{16 \times 10^{-4}}$					
u	55×10^{-4}	[1182]	CMS	8 TeV	$19.7\,\mathrm{fb}^{-1}$	multilepton, $\gamma\gamma$, $b\bar{b}$
c	40×10^{-4}					
u	47×10^{-4}	[1183]	CMS	13 TeV	$35.9\,\mathrm{fb}^{-1}$	$b\bar{b}$
c	47×10^{-4}					

[HL/HE-LHC yellow report]

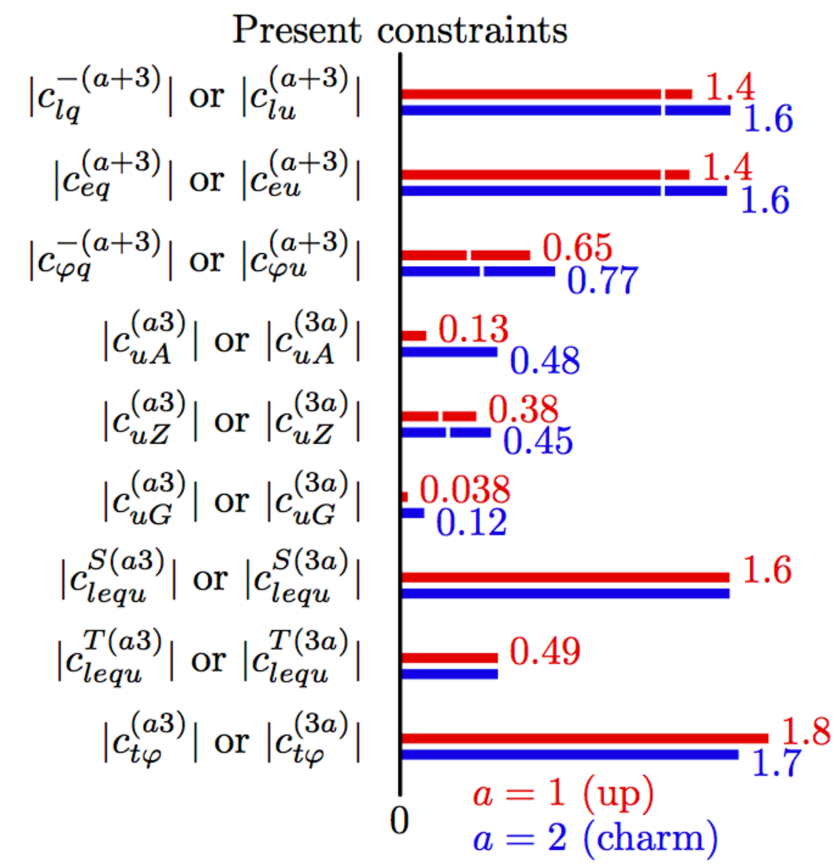

[Durieux, Kitahara, CZ '18]

Top FCNC: HL-LHC (HL/HE-LHC YR)

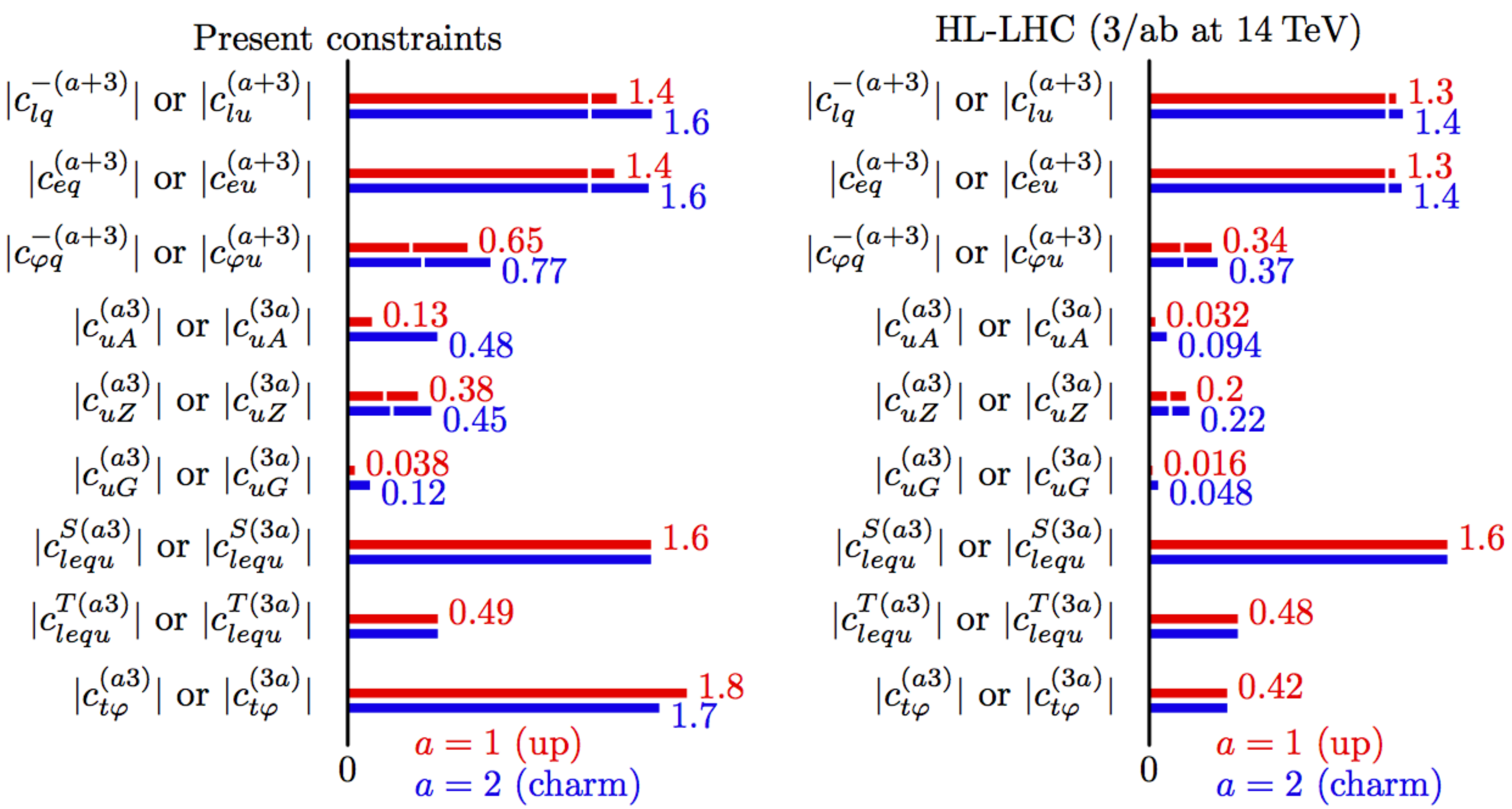

Top FCNC: FCC-ee
(Talk by F. Blekman, EPSHEP2019)

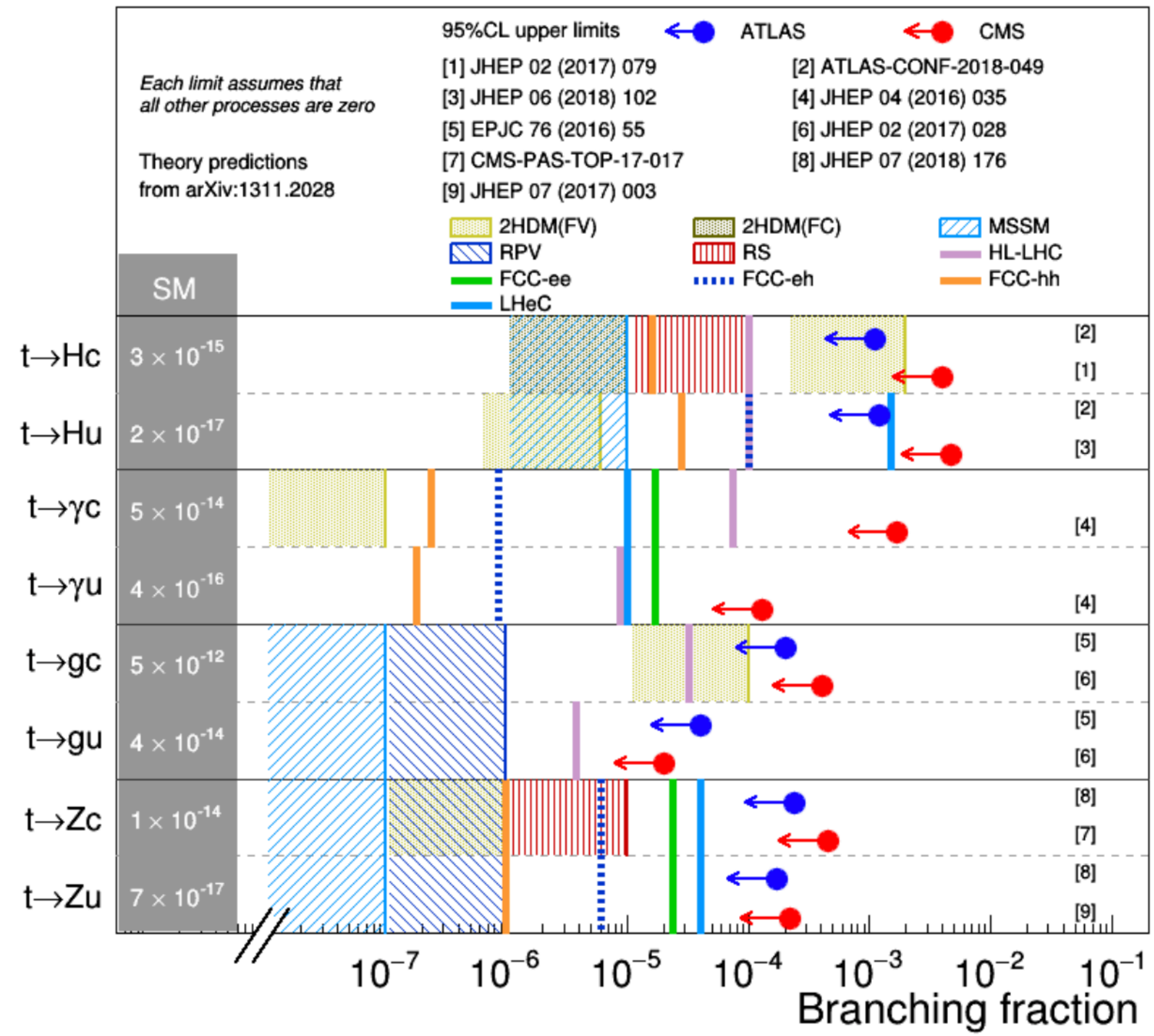

Top FCNC: CLIC YR (G. Durieux)

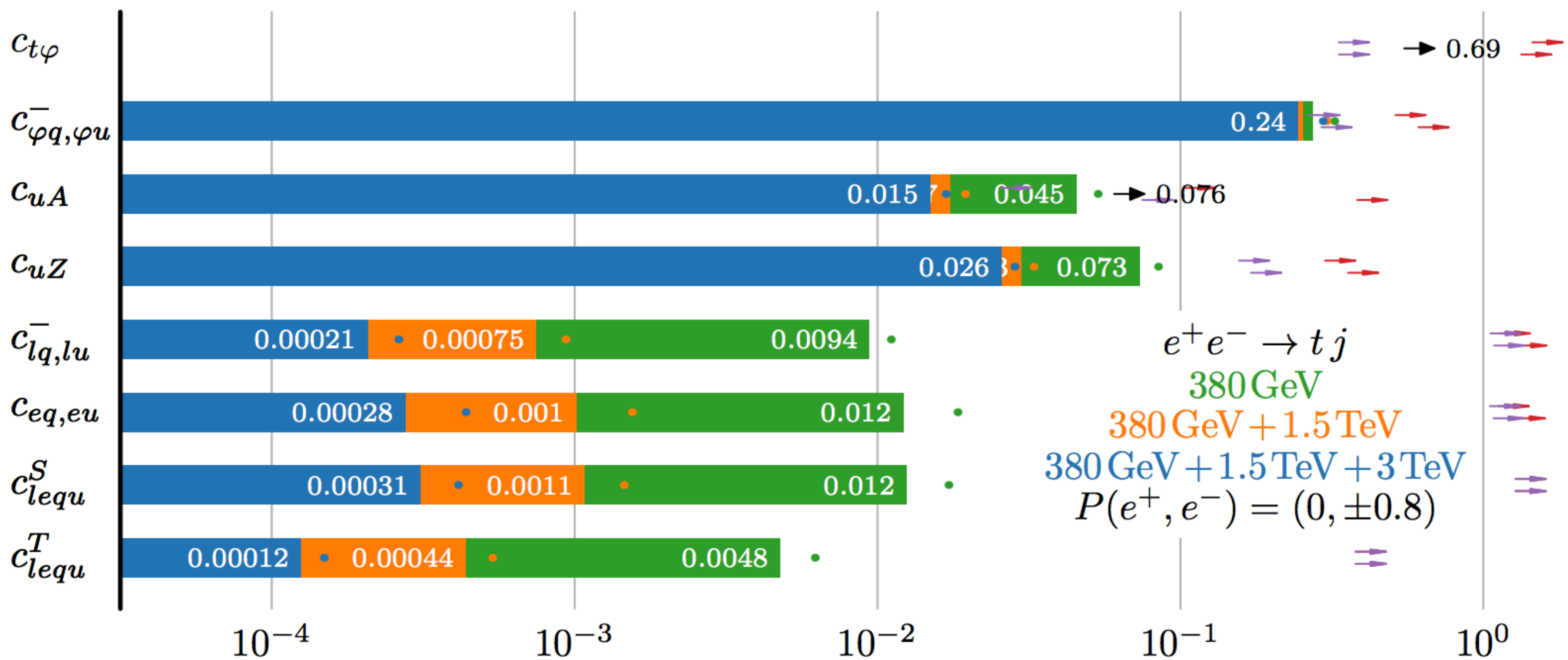

Figure 38: The expected 95% C.L. limits on top-quark FCNC operator coefficients from $e^+e^- \to t\,j$ production, with top decaying semi-leptonically, for integrated luminosities of 500 fb^{-1} (green), or in addition 1.5 ab^{-1} (orange) and 3 ab^{-1} (blue) at centre-of-mass energies of 380 GeV, 1.5 TeV and 3 TeV, respectively, and equally shared between $P(e^+, e^-) = (0, \pm 0.8)$ polarizations. The constraints from bounds on $\text{BR}(t \to j\gamma)$ and $\text{BR}(t \to jh)$, Section 3.4.2, are indicated with black arrows. Small dots indicate the limits obtained without beam polarization. Current LHC limits and the projected HL-LHC reach obtained in Ref. [139] are reported as red and purple arrows, respectively. Upper (lower) ones stand for top-up (top-charm) FCNCs.

Top FCNC

[Aguilar-Saavedra et al. '18]
[G. Durieux, the CLIC Potential for New Physics, Sec. 3.1.2, '18]

Warsaw basis operators

[B. Grzadkowski et al. 10]

$$O^{(ij)}_{u\varphi} = \bar{q}_i u_j \tilde{H}\,(H^\dagger H),$$
$$O^{1(ij)}_{\varphi q} = (H^\dagger i\overleftrightarrow{D}_\mu H)(\bar{q}_i \gamma^\mu q_j),$$
$$O^{3(ij)}_{\varphi q} = (H^\dagger i\overleftrightarrow{D}^I_\mu H)(\bar{q}_i \gamma^\mu \tau^I q_j),$$
$$O^{(ij)}_{\varphi u} = (H^\dagger i\overleftrightarrow{D}_\mu H)(\bar{u}_i \gamma^\mu u_j),$$
$$O^{(ij)}_{\varphi ud} = (\tilde{H}^\dagger i D_\mu H)(\bar{u}_i \gamma^\mu d_j),$$
$$O^{(ij)}_{uW} = (\bar{q}_i \sigma^{\mu\nu} \tau^I u_j)\,\tilde{H} W^I_{\mu\nu}$$
$$O^{(ij)}_{dW} = (\bar{q}_i \sigma^{\mu\nu} \tau^I d_j)\,H W^I_{\mu\nu},$$
$$O^{(ij)}_{uB} = (\bar{q}_i \sigma^{\mu\nu} u_j) \tilde{H} B_{\mu\nu},$$
$$O^{(ij)}_{uG} = (\bar{q}_i \sigma^{\mu\nu} T^A u_j)\,\tilde{H} G^A_{\mu\nu}.$$
$$O^{1(ijkl)}_{lq} = (\bar{l}_i \gamma^\mu l_j)(\bar{q}_k \gamma^\mu q_l),$$
$$O^{3(ijkl)}_{lq} = (\bar{l}_i \gamma^\mu \tau^I l_j)(\bar{q}_k \gamma^\mu \tau^I q_l),$$
$$O^{(ijkl)}_{lu} = (\bar{l}_i \gamma^\mu l_j)(\bar{u}_k \gamma^\mu u_l),$$
$$O^{(ijkl)}_{eq} = (\bar{e}_i \gamma^\mu e_j)(\bar{q}_k \gamma^\mu q_l),$$
$$O^{(ijkl)}_{eu} = (\bar{e}_i \gamma^\mu e_j)(\bar{u}_k \gamma^\mu u_l),$$
$$O^{1(ijkl)}_{lequ} = (\bar{l}_i e_j)\;\varepsilon\;(\bar{q}_k u_l),$$
$$O^{3(ijkl)}_{lequ} = (\bar{l}_i \sigma^{\mu\nu} e_j)\;\varepsilon\;(\bar{q}_k \sigma_{\mu\nu} u_l),$$
$$O^{(ijkl)}_{ledq} = (\bar{l}_i e_j (\bar{d}_k q_l)(\bar{u}_k \gamma^\mu u_l),$$

Relevant D.o.F for tops

[Aguilar-Saavedra et al. '18]

$$c^{-[I](3+a)}_{\varphi q} \equiv {}^{[\Im]}_{\Re}\{C^{1(3a)}_{\varphi q} - C^{3(3a)}_{\varphi q}\},$$
$$c^{[I](3+a)}_{\varphi u} \equiv {}^{[\Im]}_{\Re}\{C^{(3a)}_{\varphi u}\},$$
$$c^{[I](3a)}_{uA} \equiv {}^{[\Im]}_{\Re}\{c_W C^{(3a)}_{uB} + s_W C^{(3a)}_{uW}\},$$
$$c^{[I](a3)}_{uA} \equiv {}^{[\Im]}_{\Re}\{c_W C^{(a3)}_{uB} + s_W C^{(a3)}_{uW}\},$$
$$c^{[I](3a)}_{uZ} \equiv {}^{[\Im]}_{\Re}\{-s_W C^{(3a)}_{uB} + c_W C^{(3a)}_{uW}\},$$
$$c^{[I](a3)}_{uZ} \equiv {}^{[\Im]}_{\Re}\{-s_W C^{(a3)}_{uB} + c_W C^{(a3)}_{uW}\},$$
$$c^{-[I](1,3+a)}_{lq} \equiv {}^{[\Im]}_{\Re}\{C^{-(113a)}_{lq}\},$$
$$c^{[I](1,3+a)}_{eq} \equiv {}^{[\Im]}_{\Re}\{C^{(113a)}_{eq}\},$$
$$c^{[I](1,3+a)}_{lu} \equiv {}^{[\Im]}_{\Re}\{C^{(113a)}_{lu}\},$$
$$c^{[I](1,3+a)}_{eu} \equiv {}^{[\Im]}_{\Re}\{C^{(113a)}_{eu}\},$$
$$c^{S[I](1,3a)}_{lequ} \equiv {}^{[\Im]}_{\Re}\{C^{1(113a)}_{lequ}\},$$
$$c^{S[I](1,a3)}_{lequ} \equiv {}^{[\Im]}_{\Re}\{C^{1(11a3)}_{lequ}\},$$
$$c^{T[I](1,3a)}_{lequ} \equiv {}^{[\Im]}_{\Re}\{C^{3(113a)}_{lequ}\},$$
$$c^{T[I](1,a3)}_{lequ} \equiv {}^{[\Im]}_{\Re}\{C^{3(11a3)}_{lequ}\}.$$

No interference between rows, sufficient to focus on 7 parameters at a time

28 DoFs relevant for ee->tj

CP even:

$$c^{-(1,3+a)}_{lq},\quad c^{(1,3+a)}_{eq},\quad c^{-(3+a)}_{\varphi q},\quad c^{(a3)}_{uA},\quad c^{(a3)}_{uZ},\quad c^{S(1,a3)}_{lequ},\quad c^{T(1,a3)}_{lequ},$$
$$c^{(1,3+a)}_{lu},\quad c^{(1,3+a)}_{eu},\quad c^{(3+a)}_{\varphi u},\quad c^{(3a)}_{uA},\quad c^{(3a)}_{uZ},\quad c^{S(1,3a)}_{lequ},\quad c^{T(1,3a)}_{lequ},$$

CP odd:

$$c^{-I(1,3+a)}_{lq},\quad c^{I(1,3+a)}_{eq},\quad c^{-I(3+a)}_{\varphi q},\quad c^{I(a3)}_{uA},\quad c^{I(a3)}_{uZ},\quad c^{SI(1,a3)}_{lequ},\quad c^{TI(1,a3)}_{lequ},$$
$$c^{I(1,3+a)}_{lu},\quad c^{I(1,3+a)}_{eu},\quad c^{I(3+a)}_{\varphi u},\quad c^{I(3a)}_{uA},\quad c^{I(3a)}_{uZ},\quad c^{SI(1,3a)}_{lequ},\quad c^{TI(1,3a)}_{lequ},$$

Left-handed q

Right-handed q

a=1: tuV/tull
a=2: tcV/tcll

Top FCNC: 2-fermion operators

28 DoFs relevant for ee

$c_{\varphi q}^{-(3+a)}$,	$c_{uA}^{(a3)}$,	$c_{uZ}^{(a3)}$,	$c_{lequ}^{S(1,a3)}$,	$c_{lequ}^{T(1,a3)}$,	$c_{lq}^{-(1,3+a)}$,	$c_{eq}^{(1,3+a)}$,
$c_{\varphi u}^{(3+a)}$,	$c_{uA}^{(3a)}$,	$c_{uZ}^{(3a)}$,	$c_{lequ}^{S(1,3a)}$,	$c_{lequ}^{T(1,3a)}$,	$c_{lu}^{(1,3+a)}$,	$c_{eu}^{(1,3+a)}$,
$c_{\varphi q}^{-I(3+a)}$,	$c_{uA}^{I(a3)}$,	$c_{uZ}^{I(a3)}$,	$c_{lequ}^{SI(1,a3)}$,	$c_{lequ}^{TI(1,a3)}$,	$c_{lq}^{-I(1,3+a)}$,	$c_{eq}^{I(1,3+a)}$
$c_{\varphi u}^{I(3+a)}$,	$c_{uA}^{I(3a)}$,	$c_{uZ}^{I(3a)}$	$c_{lequ}^{SI(1,3a)}$,	$c_{lequ}^{TI(1,3a)}$,	$c_{lu}^{I(1,3+a)}$,	$c_{eu}^{I(1,3+a)}$

2-fermion FCNC

$$\bar{q}\gamma^{\mu}q \quad \varphi^{\dagger} i\overleftrightarrow{D}_{\mu}\varphi,$$
$$\bar{q}\gamma^{\mu}\tau^{I}q \quad \varphi^{\dagger} i\overleftrightarrow{D}^{I}_{\mu}\varphi,$$
$$\bar{u}\gamma^{\mu}u \quad \varphi^{\dagger} i\overleftrightarrow{D}_{\mu}\varphi,$$
$$\bar{q}\sigma^{\mu\nu}u\,\tilde{\varphi} \quad B_{\mu\nu},$$
$$\bar{q}\sigma^{\mu\nu}\tau^{I}u\,\tilde{\varphi} \quad W^{I}_{\mu\nu},$$

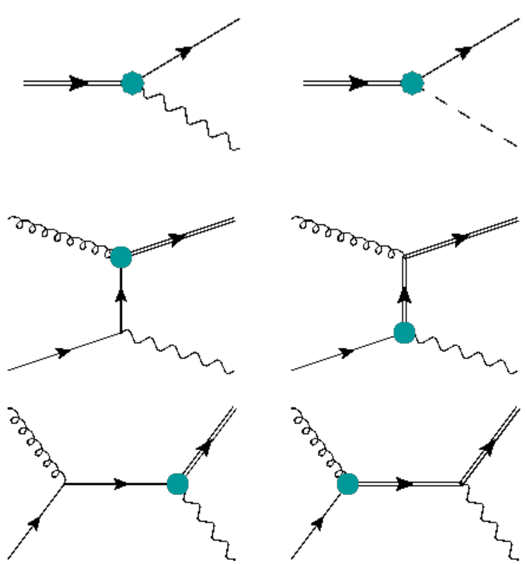

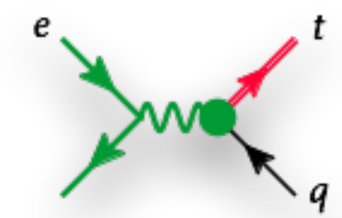

FCC-ee: [H. Khanpour et al. 1408.2090]

Integrated luminosity	Branching ratio	240 GeV	350 GeV	500 GeV
300 fb^{-1}	$Br(t \to q\gamma)$	1.23×10^{-4}	3.43×10^{-5}	2.45×10^{-5}
	$Br(t \to qZ)$ $(\sigma_{\mu\nu})$	1.50×10^{-4}	4.97×10^{-5}	3.94×10^{-5}
	$Br(t \to qZ)$ (γ_{μ})	3.06×10^{-4}	1.83×10^{-4}	2.67×10^{-4}
3 ab^{-1}	$Br(t \to q\gamma)$	3.70×10^{-5}	9.86×10^{-6}	6.76×10^{-6}
	$Br(t \to qZ)$ $(\sigma_{\mu\nu})$	4.50×10^{-5}	1.41×10^{-5}	1.09×10^{-5}
	$Br(t \to qZ)$ (γ_{μ})	9.25×10^{-5}	5.27×10^{-5}	7.49×10^{-4}
10 ab^{-1}	$Br(t \to q\gamma)$	2.01×10^{-5}	5.25×10^{-6}	3.59×10^{-6}
	$Br(t \to qZ)$ $(\sigma_{\mu\nu})$	2.44×10^{-5}	7.60×10^{-6}	5.85×10^{-6}
	$Br(t \to qZ)$ (γ_{μ})	5.02×10^{-5}	2.83×10^{-5}	4.00×10^{-5}

ILC 500: [Aguilar–Saavedra & Riemann '01]

CLIC: [G. Durieux, the CLIC Potential for New Physics, Sec.3.1.2, 18]

Goal 1: have similar results for CEPC

Top FCNC: 4-fermion operators

28 DoFs relevant for ee

$c_{\varphi q}^{-(3+a)}$, $c_{uA}^{(a3)}$, $c_{uZ}^{(a3)}$, $c_{lequ}^{S(1,a3)}$, $c_{lequ}^{T(1,a3)}$, $c_{lq}^{-(1,3+a)}$, $c_{eq}^{(1,3+a)}$,

$c_{\varphi u}^{(3+a)}$, $c_{uA}^{(3a)}$, $c_{uZ}^{(3a)}$, $c_{lequ}^{S(1,3a)}$, $c_{lequ}^{T(1,3a)}$, $c_{lu}^{(1,3+a)}$, $c_{eu}^{(1,3+a)}$,

$c_{\varphi q}^{-I(3+a)}$, $c_{uA}^{I(a3)}$, $c_{uZ}^{I(a3)}$, $c_{lequ}^{SI(1,a3)}$, $c_{lequ}^{TI(1,a3)}$, $c_{lq}^{-I(1,3+a)}$, $c_{eq}^{I(1,3+a)}$,

$c_{\varphi u}^{I(3+a)}$, $c_{uA}^{I(3a)}$, $c_{uZ}^{I(3a)}$, $c_{lequ}^{SI(1,3a)}$, $c_{lequ}^{TI(1,3a)}$, $c_{lu}^{I(1,3+a)}$, $c_{eu}^{I(1,3+a)}$

4-fermion FCNC

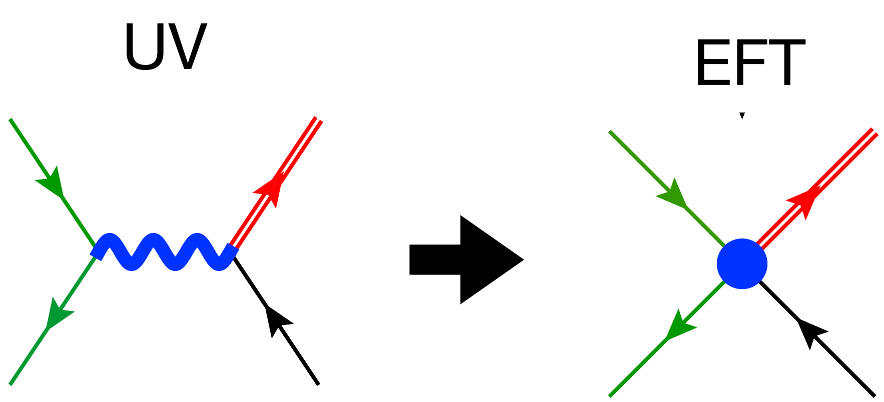

$$\mathcal{L}_{tcee} = \frac{1}{\Lambda^2} \sum_{i,j=L,R} \Big[V_{ij}\,(\bar{e}\gamma_\mu P_i e)\,(\bar{t}\gamma^\mu P_j c) + S_{ij}\,(\bar{e}P_i e)\,(\bar{t}P_j c) + T_{ij}\,(\bar{e}\sigma_{\mu\nu}P_i e)\,(\bar{t}\sigma_{\mu\nu}P_j c) \Big]\,,$$

[Bar-Shalom, Wudka '99]

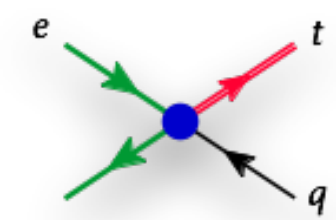

Best bounds still from LEP2!

Scenario	Hadronic topology				Semi-leptonic topology				Combined topologies			
	obs.	-1σ	exp.	$+1\sigma$	obs.	-1σ	exp.	$+1\sigma$	obs.	-1σ	exp.	$+1\sigma$
SVT	1218	1268	1180	1097	1315	1406	1301	1203	1402	1468	1366	1264
S	577	604	556	520	647	647	603	555	685	693	641	593
V	953	1003	933	863	997	1069	997	921	1073	1141	1068	980
T	1069	1117	1045	969	1124	1232	1142	1052	1204	1300	1210	1114

Table 5: Observed and expected 95% CL lower limits on Λ (GeV)

[DELPHI, CERN–PH–EP/2010–056]

CLIC: [G. Durieux, the CLIC Potential for New Physics, Sec.3.1.2, '18]

Currently no results for FCC-ee and ILC

No dedicated search (t>qll) at the LHC
(Recast from t>qZ is possible [Chala, Santiago, Spannowsky '18])

Goal 2: study 4-f operators at CEPC

Top FCNC: current/future limits

[HL/HE YR, 1812.07638]

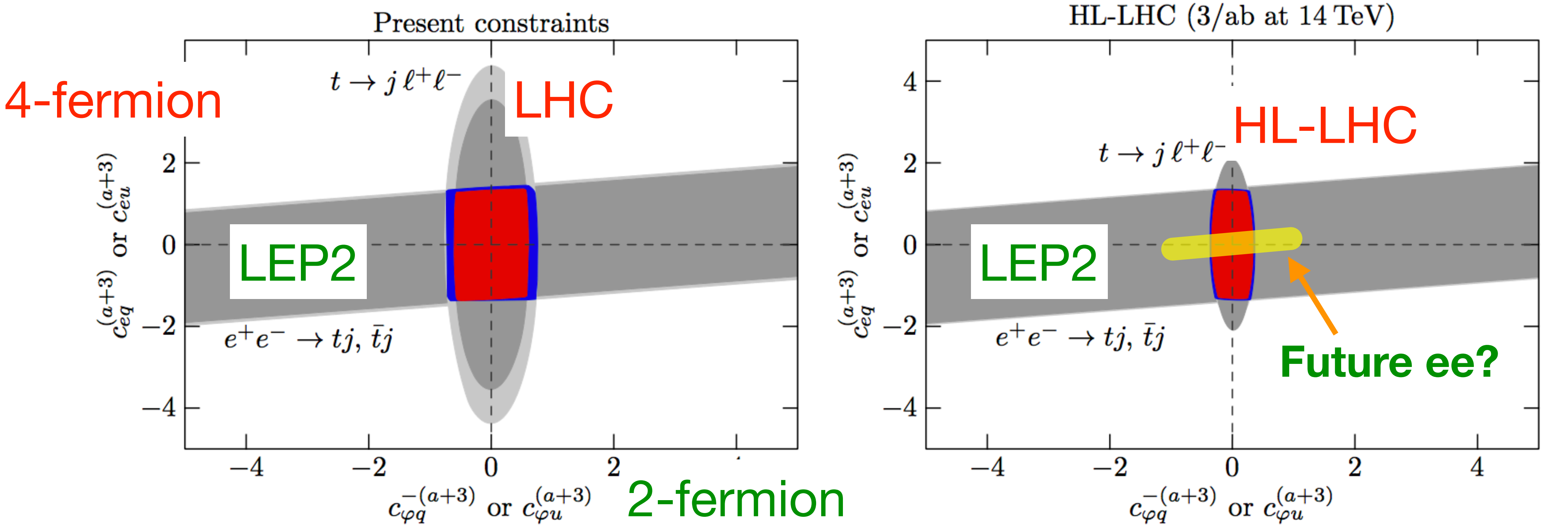

Fig. 59: Current (left) and prospective HL-LHC (right) 95% C.L. limits on top-quark FCNC operator coefficients in a two-dimensional plane formed by two- (x axis) and four-fermion (y axis) operator coefficients. Other parameters are marginalized over, within the constraints obtained when all measurements are included. Red and blue regions are the combined constraints for top-up and top-charm FCNCs. The impact of $t \to j\ell^+\ell^-$ and $e^+e^- \to tj, \bar{t}j$ measurements is displayed separately in dark and light gray colors for top-up and top-charm FCNCs, respectively.

Goal 3: confirm the same complementarity between HL-LHC and CEPC

LHC

ee collider

2-fermion OP

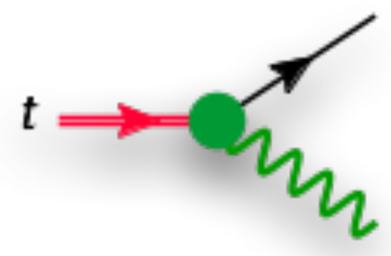

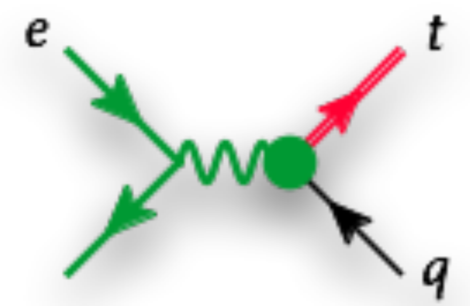

2f: 8.1e-5 GeV for $\frac{c}{\Lambda^2} = 1\ \text{TeV}^{-2}$

2f: 1.8 fb

4-fermion OP

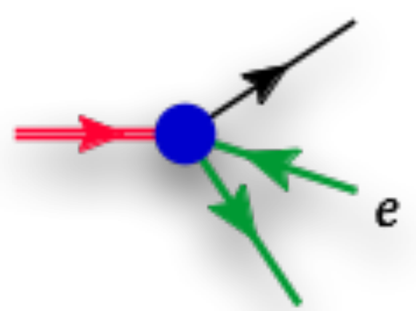

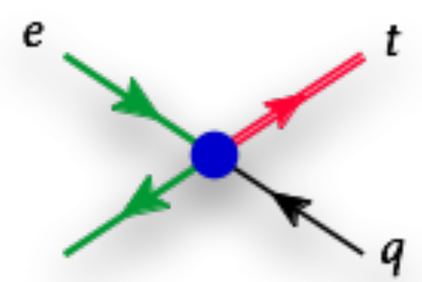

Phase space suppression

E^4/m_Z^4 scaling enhancement

4f: 3.2e-6 GeV

4f: 120 fb

The analysis

- CEPC scenario, 240 GeV, 5.6 ab^{-1}
  - Expect similar results for FCC-ee 240 GeV 5 ab^{-1}.
- LO+PS, with MadGraph5 and Pythia8
- FCNC implementation: **`dim6top`**
  https://feynrules.irmp.ucl.ac.be/wiki/dim6top
- Detector effects: Delphes with CEPC card
- Signal:

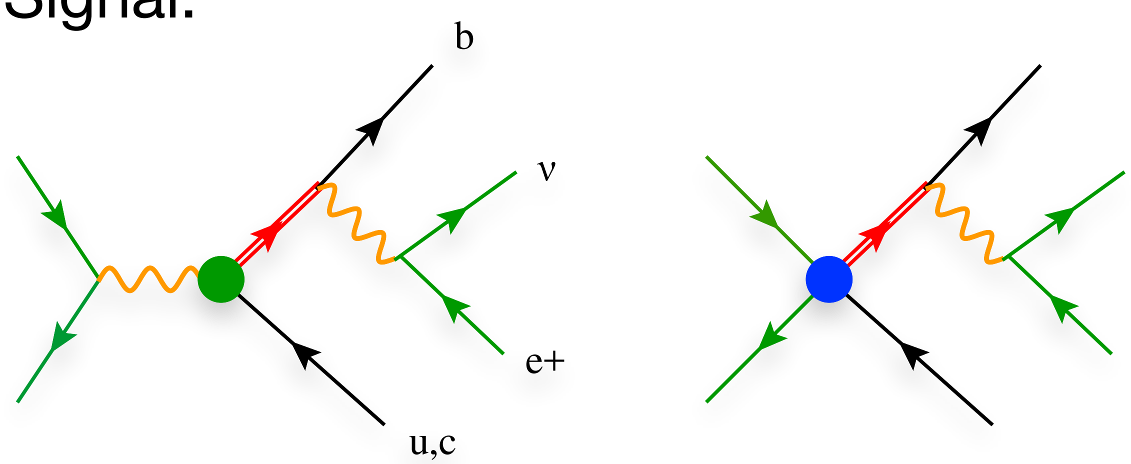

$$m_{top,rec} \approx 172.5 \text{ GeV}$$

$$E_{j,rec} \approx \frac{s - m_t^2}{2\sqrt{s}} \approx 58 \text{ GeV}$$

- Background: Wjj dominant

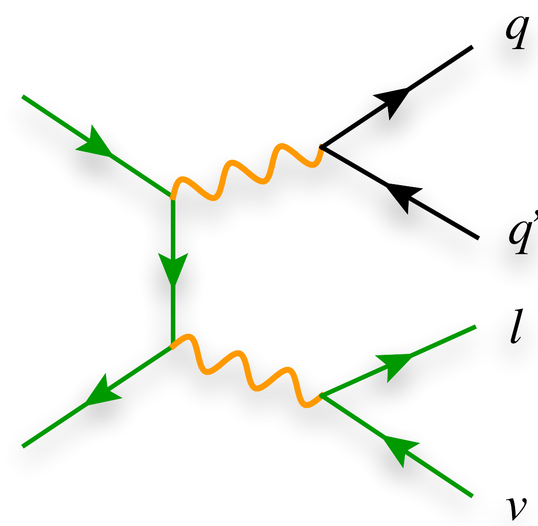

$$m_{jj} \approx 80.4 \text{ GeV}$$

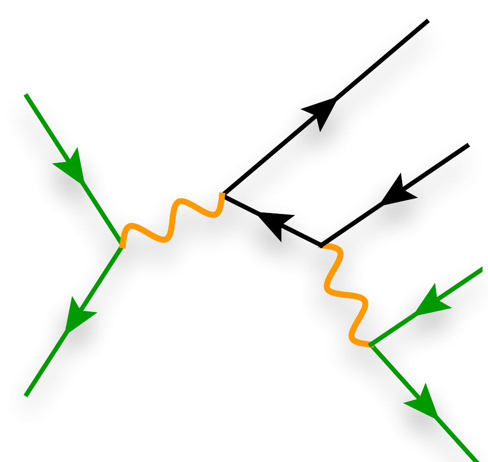

- + Zjj

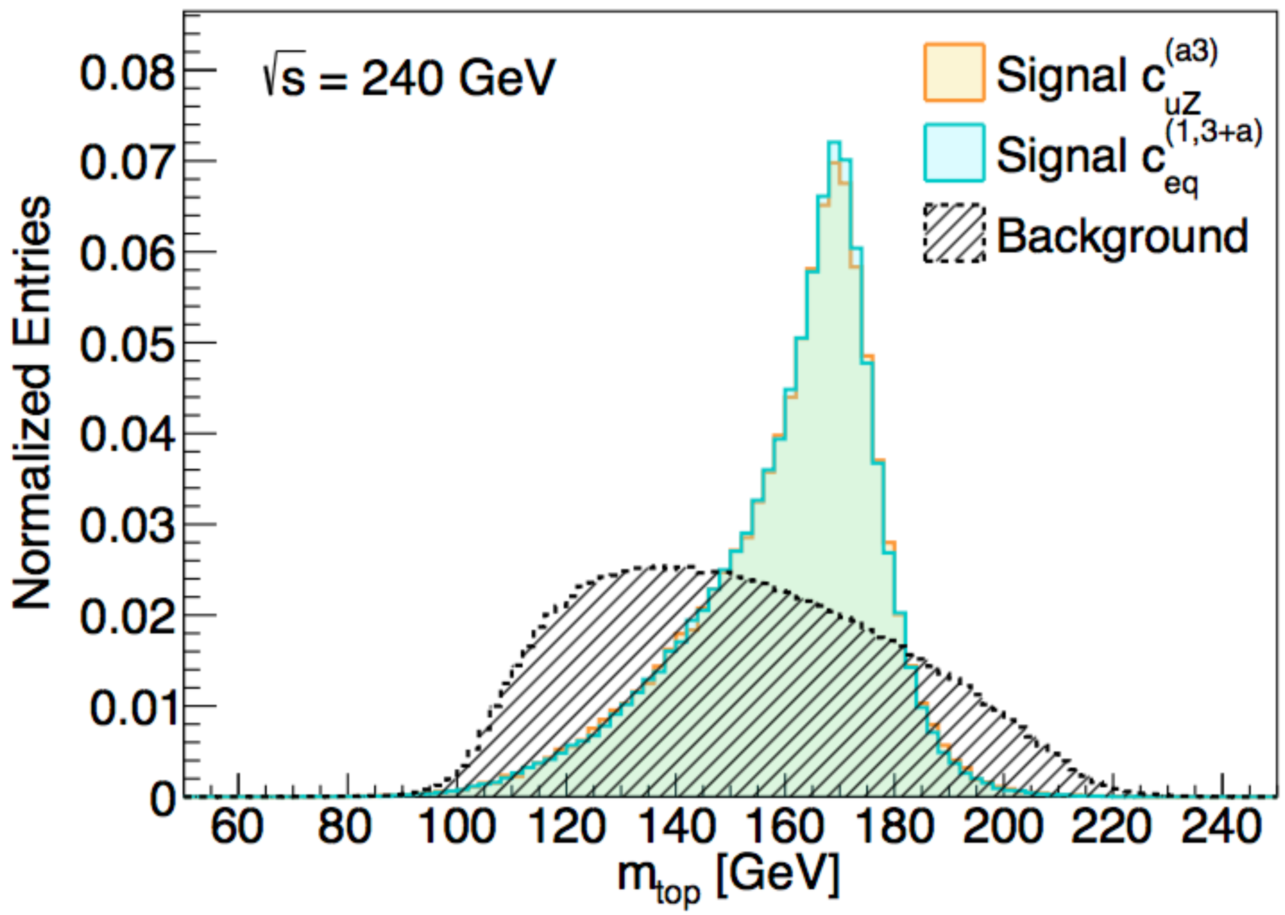

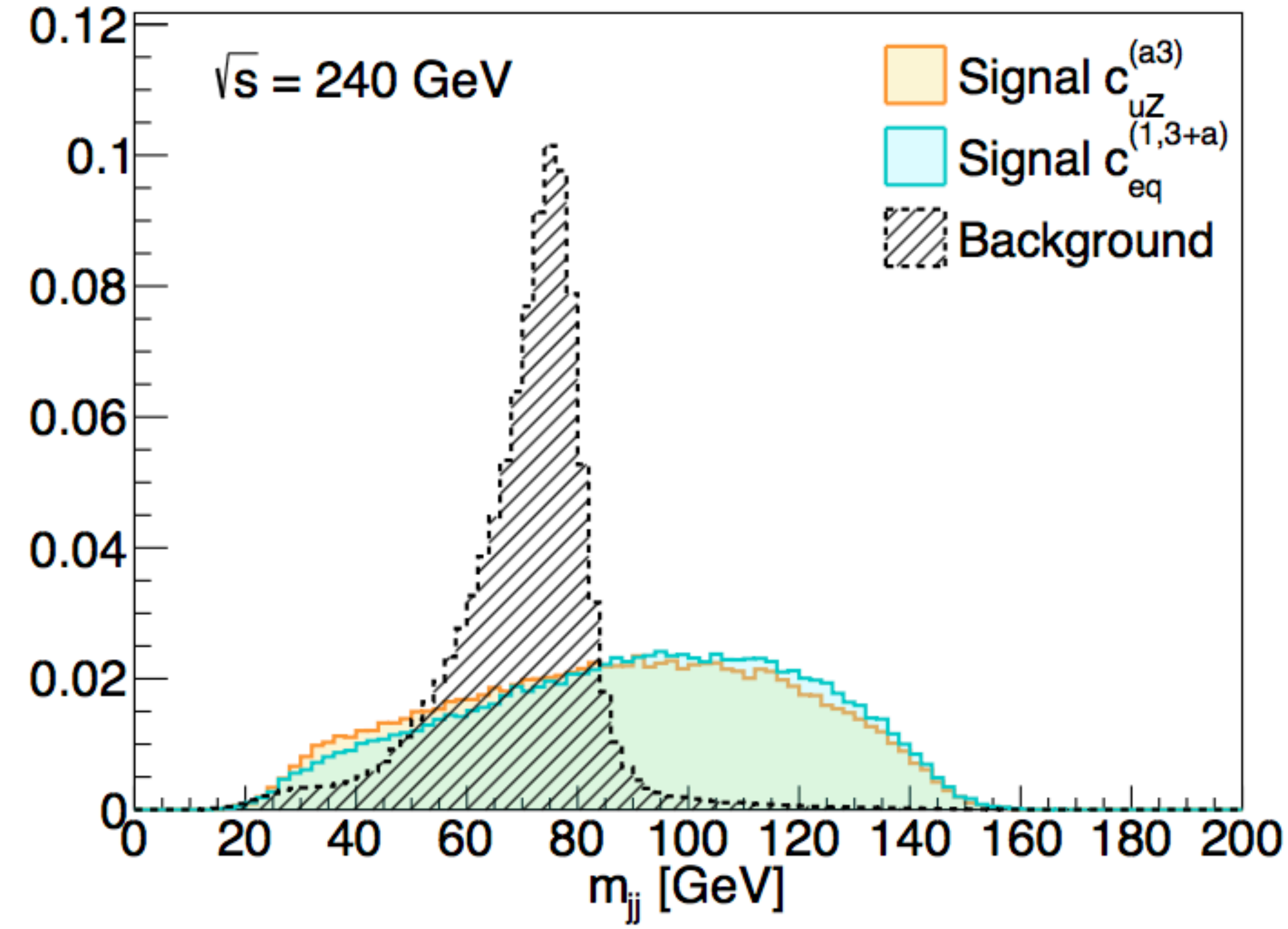

Baseline scenario: use simple cuts

$E_j < 60$ GeV , exactly 1 *b*-tagged jet

$m_{jj} > 100$ GeV ,

$m_{top} < 180$ GeV .

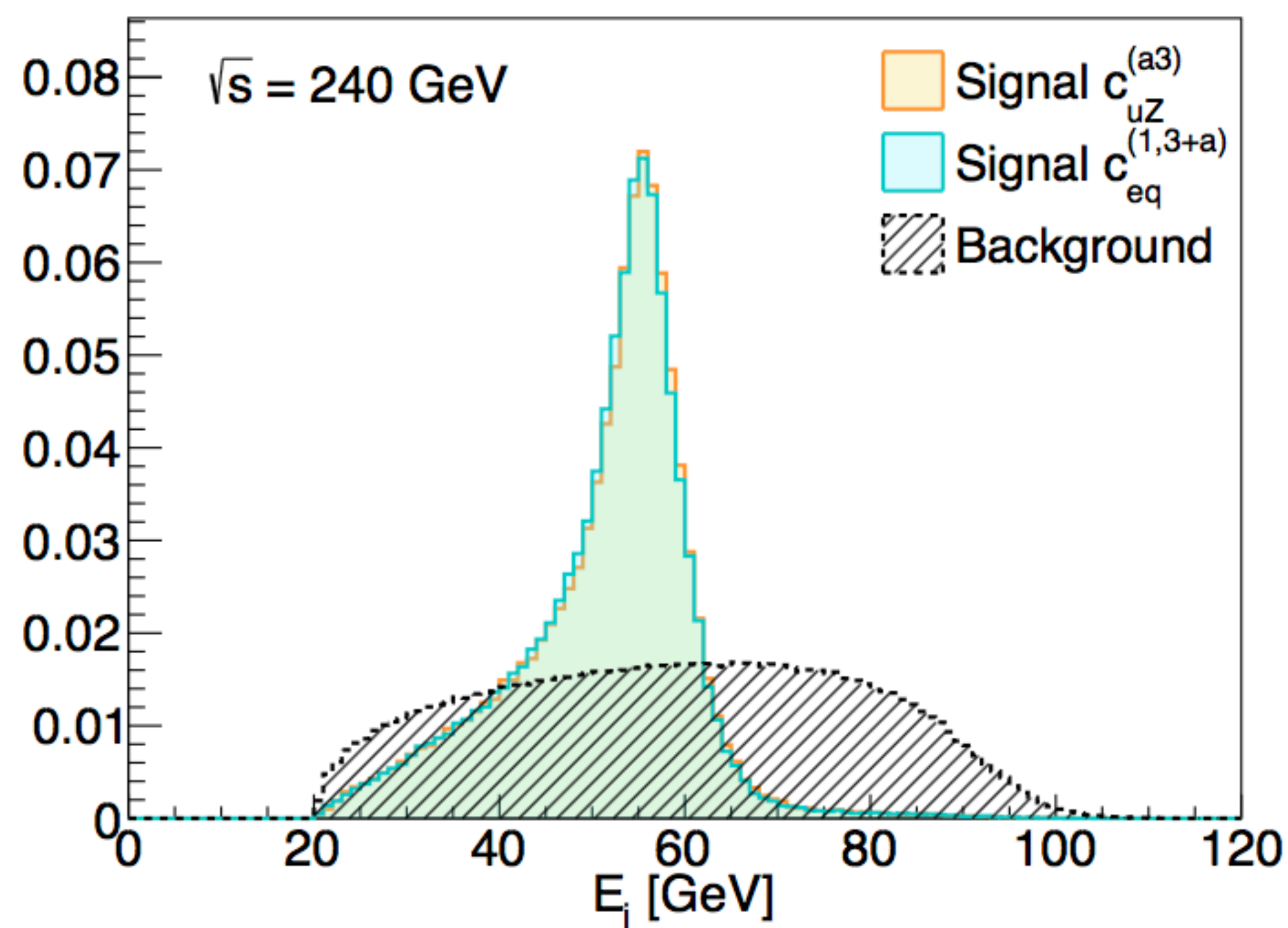

1400 events at 5.6 ab-1
-> 95% CL limit on xsec: 0.0134 fb

Needs to be translated to operators coefs…

EFT parameter space

28 DoFs relevant for ee->tj

$c_{lq}^{-(1,3+a)}$,	$c_{eq}^{(1,3+a)}$,	$c_{\varphi q}^{-(3+a)}$,	$c_{uA}^{(a3)}$,	$c_{uZ}^{(a3)}$,	$c_{lequ}^{S(1,a3)}$,	$c_{lequ}^{T(1,a3)}$,
$c_{lu}^{(1,3+a)}$,	$c_{eu}^{(1,3+a)}$,	$c_{\varphi u}^{(3+a)}$,	$c_{uA}^{(3a)}$,	$c_{uZ}^{(3a)}$,	$c_{lequ}^{S(1,3a)}$,	$c_{lequ}^{T(1,3a)}$,
$c_{lq}^{-I(1,3+a)}$,	$c_{eq}^{I(1,3+a)}$,	$c_{\varphi q}^{-I(3+a)}$,	$c_{uA}^{I(a3)}$,	$c_{uZ}^{I(a3)}$,	$c_{lequ}^{SI(1,a3)}$,	$c_{lequ}^{TI(1,a3)}$,
$c_{lu}^{I(1,3+a)}$,	$c_{eu}^{I(1,3+a)}$,	$c_{\varphi u}^{I(3+a)}$,	$c_{uA}^{I(3a)}$,	$c_{uZ}^{I(3a)}$,	$c_{lequ}^{SI(1,3a)}$,	$c_{lequ}^{TI(1,3a)}$,

$$\sigma_{\text{signal}} = \sum_{1\leq i\leq j\leq 7} \frac{C_i C_j}{\Lambda^4}\sigma_{ij}$$

- σ_{ij} : 7×8÷2=28 independent terms.
- They are determined by simulating the signal at 28 sampling points in the 7-D parameter space and fitting to a polynomial.
- With these, the limit on xsec is converted to 95% 7-D bound in the dim-6 parameter space.

Bounds on individual operators

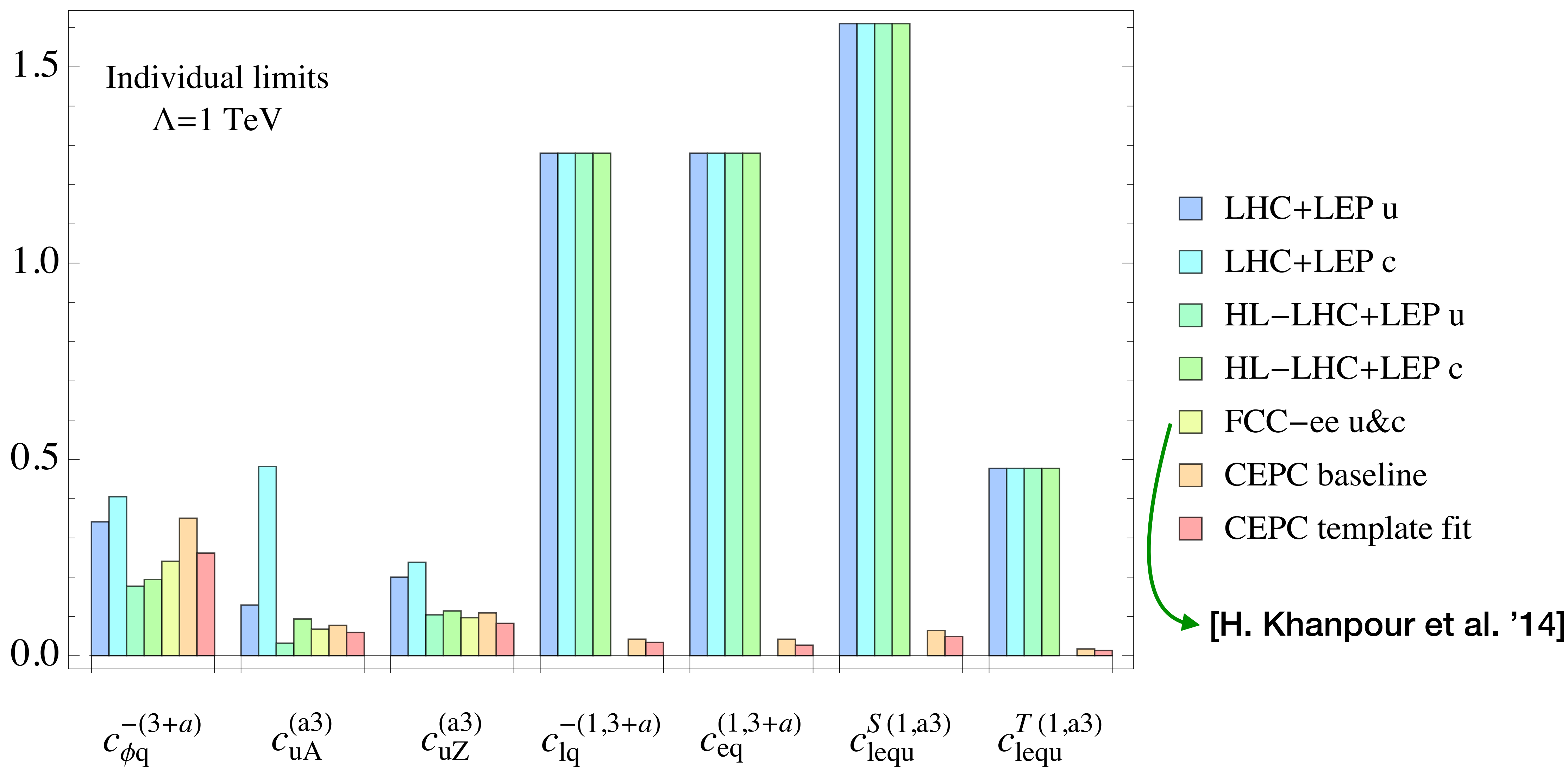

FCC-ee: 4f operator limits are not available; 2f slightly better **[H. Khanpour et al. ’14]**

CLIC: 380 GeV run + polarization, 3~4 times better on 4f

Larger energy -> better limits **[G. Durieux, the CLIC Potential for New Physics, CERN YR, 18]**

LHeC: similar limits **[W. Liu, H. Sun 1906.04884]**

Bounds on individual operators

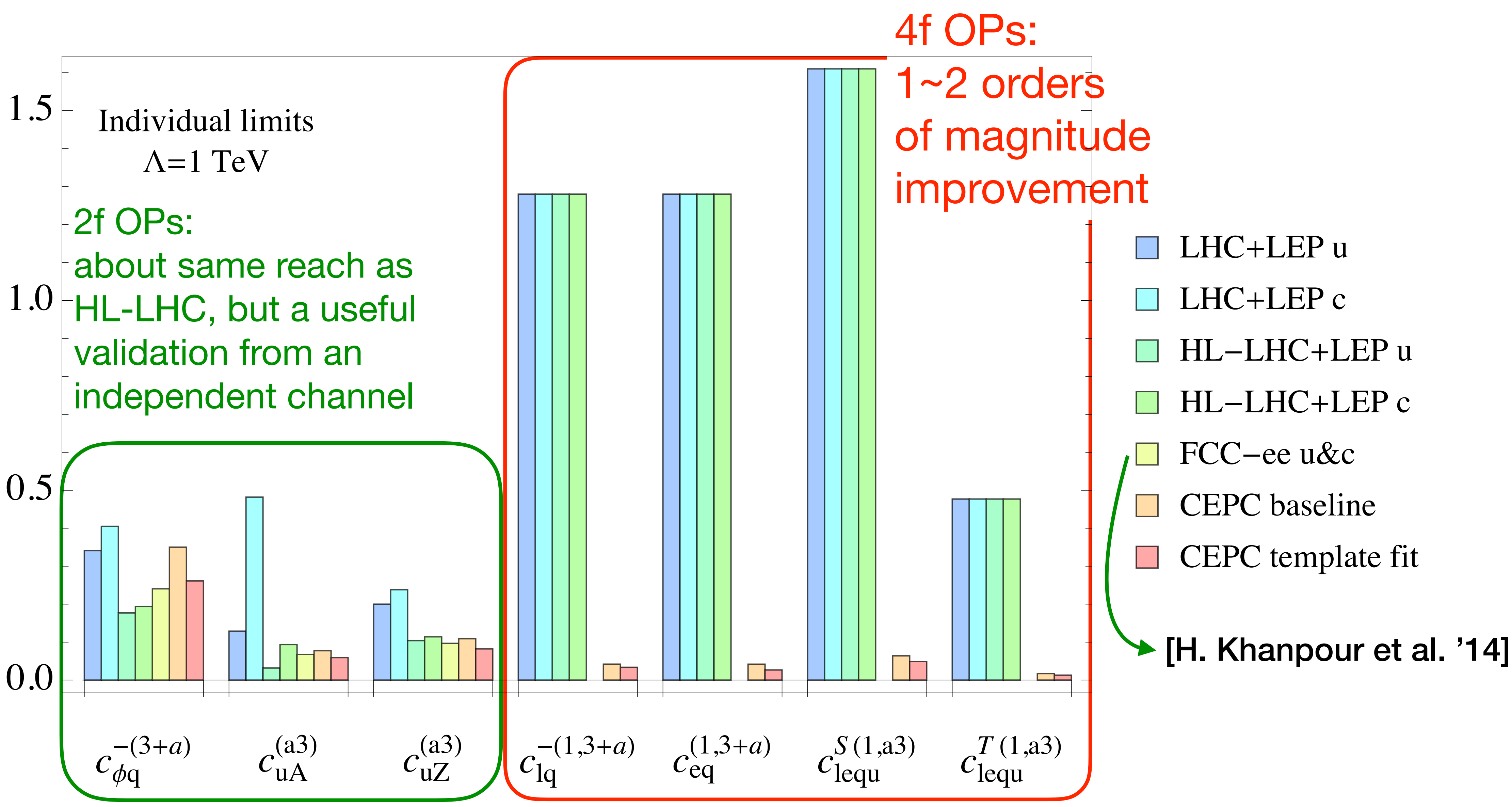

FCC-ee: 4f operator limits are not available; 2f slightly better [H. Khanpour et al. '14]

CLIC: 380 GeV run + polarization, 3~4 times better on 4f

Larger energy -> better limits [G. Durieux, the CLIC Potential for New Physics, CERN YR, 18]

LHeC: similar limits [W. Liu, H. Sun 1906.04884]

Bounds on 2f vs 4f operators: HL-LHC + CEPC

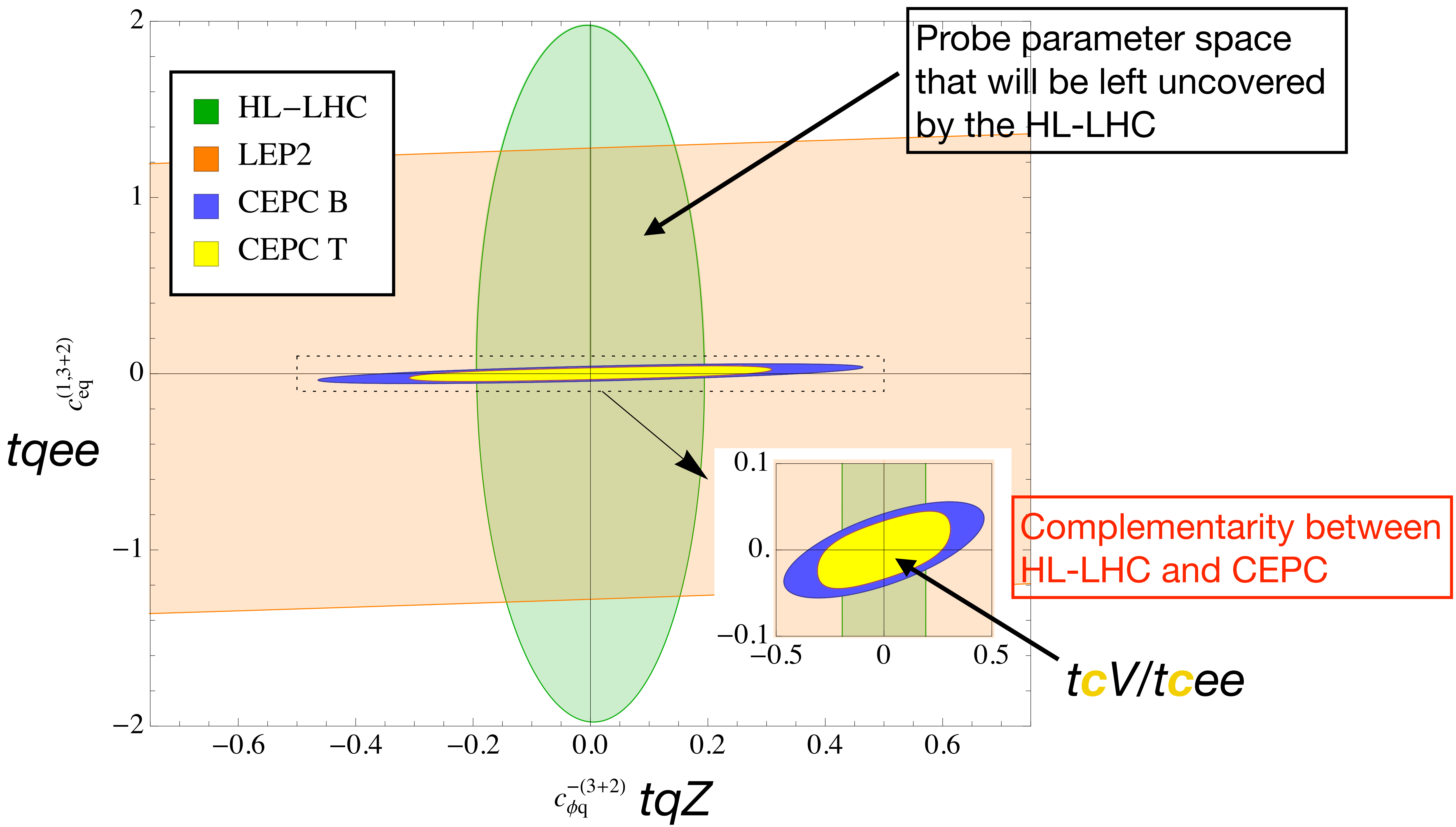

Improving with a “template fit”

- To further improve, we also consider:
  - Angular distribution:

    Signal produced by different operators with different Lorentz structures can be distinguished by production angle

➡ **This will improve the discrimination power** between different operators

  - Charm tagging: (has been mentioned in [H. Khanpour et al. 1408.2090])

    For tcV/tcee operators, the signal is ***b,c,l,v*** while the main background is ***c,s,l,v*** where the c fakes the b. So choosing a c-tagged jet improves S/B.

➡ **This will improve sensitivity on a=2 operators.** (i.e. t**c**V/t**c**ee)

Angular distribution

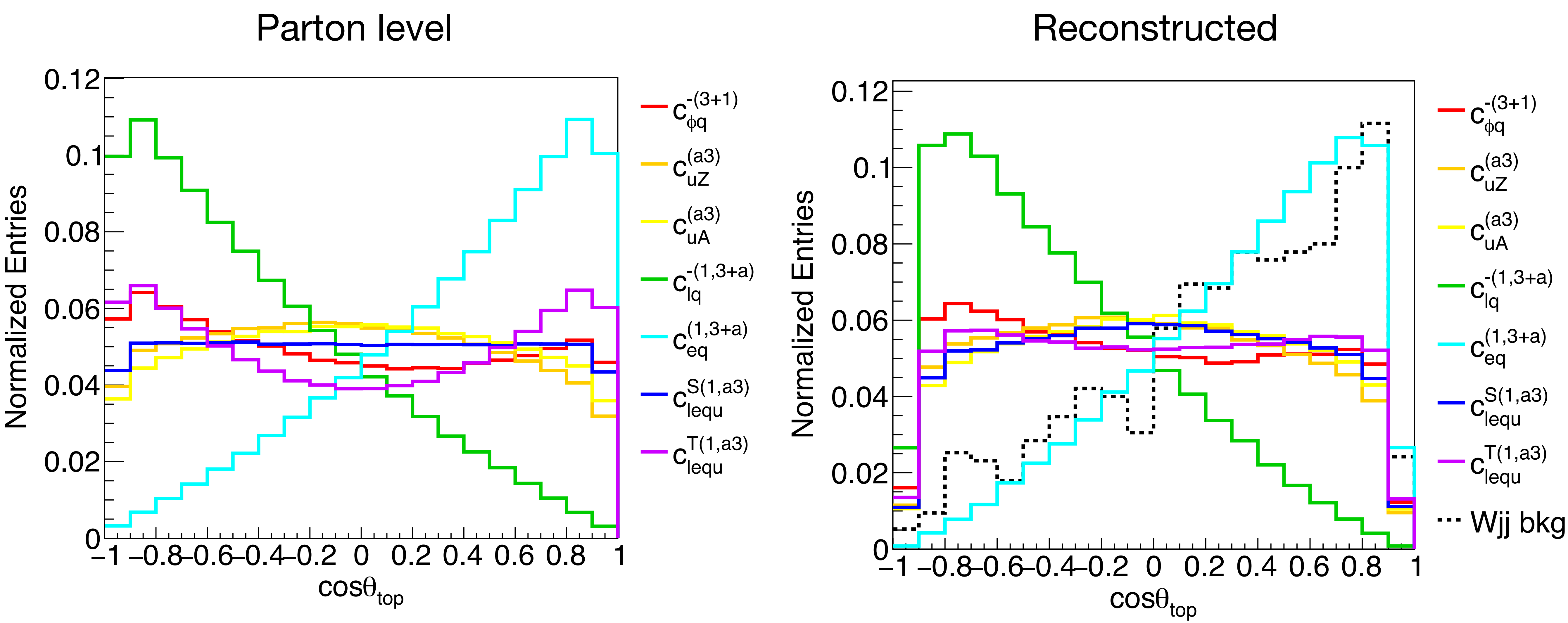

Template fit: divide the signal region into 8 bins,

i.e. 4 bins in $Q_l \times \cos\theta_{top}$ + charm tagging

Improvement from c-jet tagging

If no signal is observed:

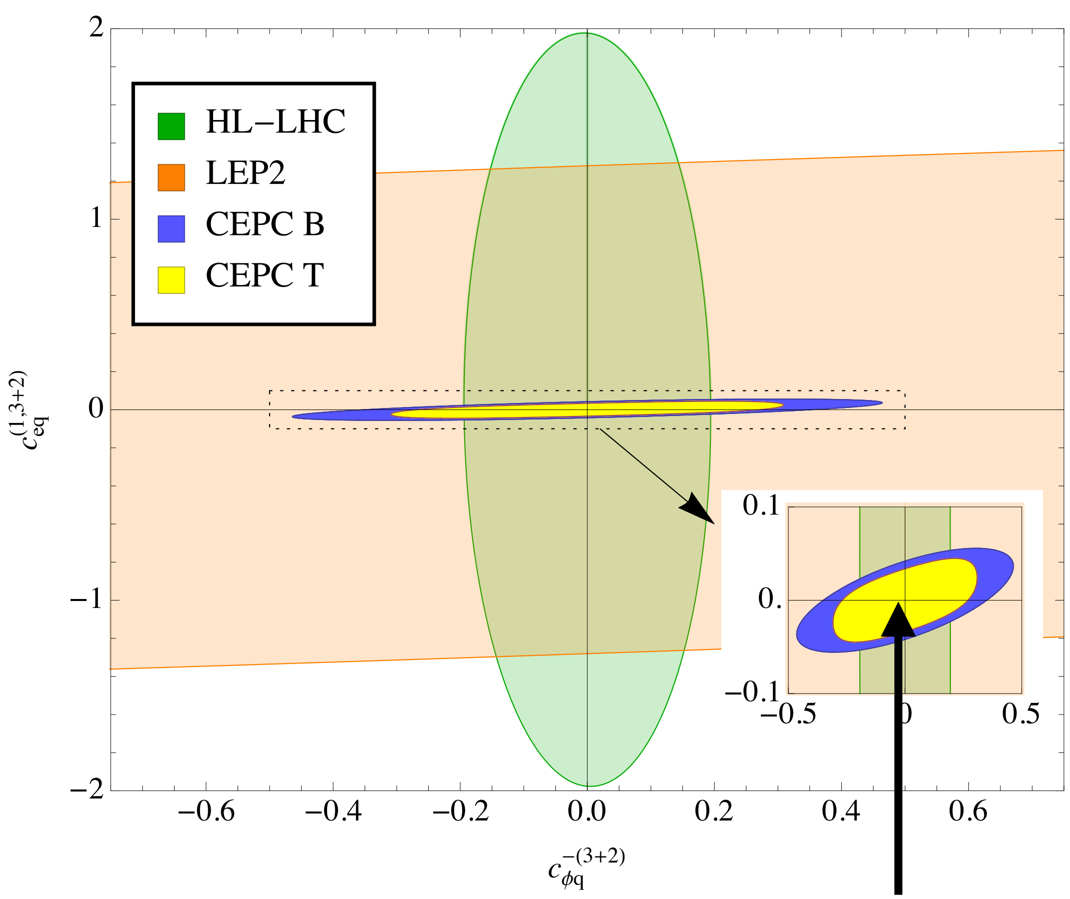

tcV/tcee

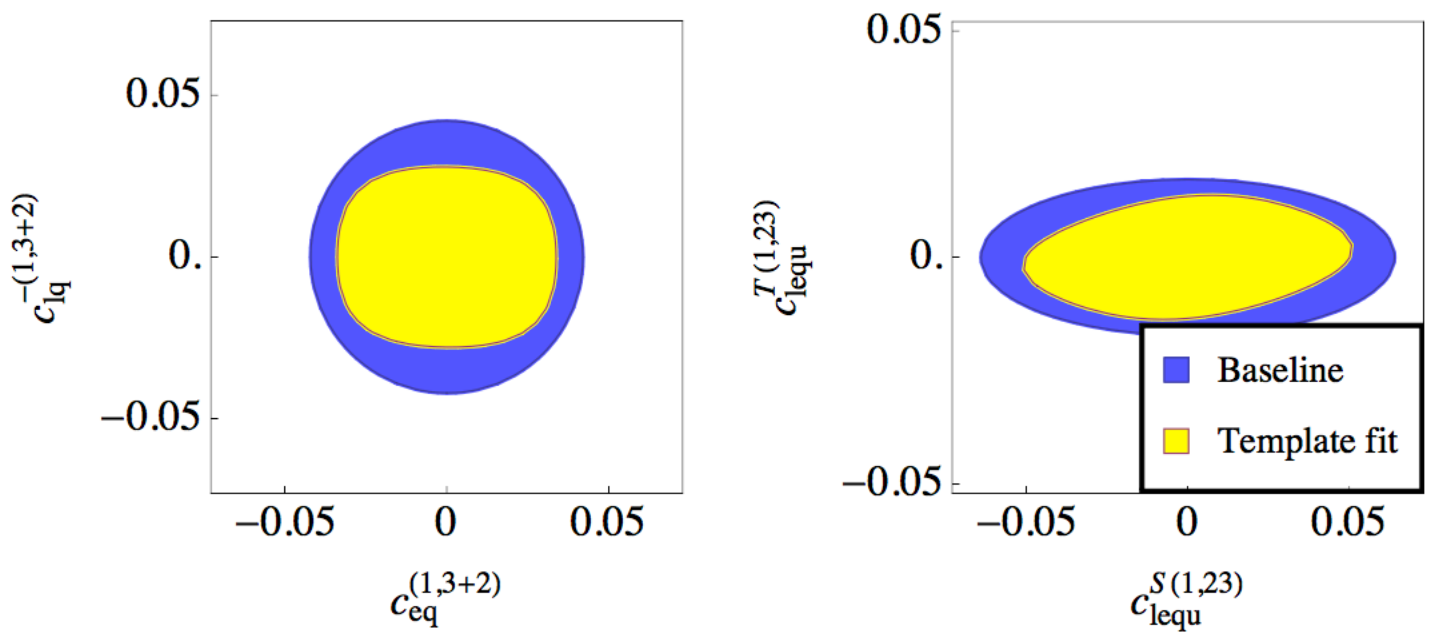

Fig. 8. Two-dimensional limits on four-fermion coefficients, at 95% CL, under the SM hypothesis, with other coefficients turned off. The template fit approach improves the sensitivity.

Discriminating between different operators, when an excess is observed

Using angular observable

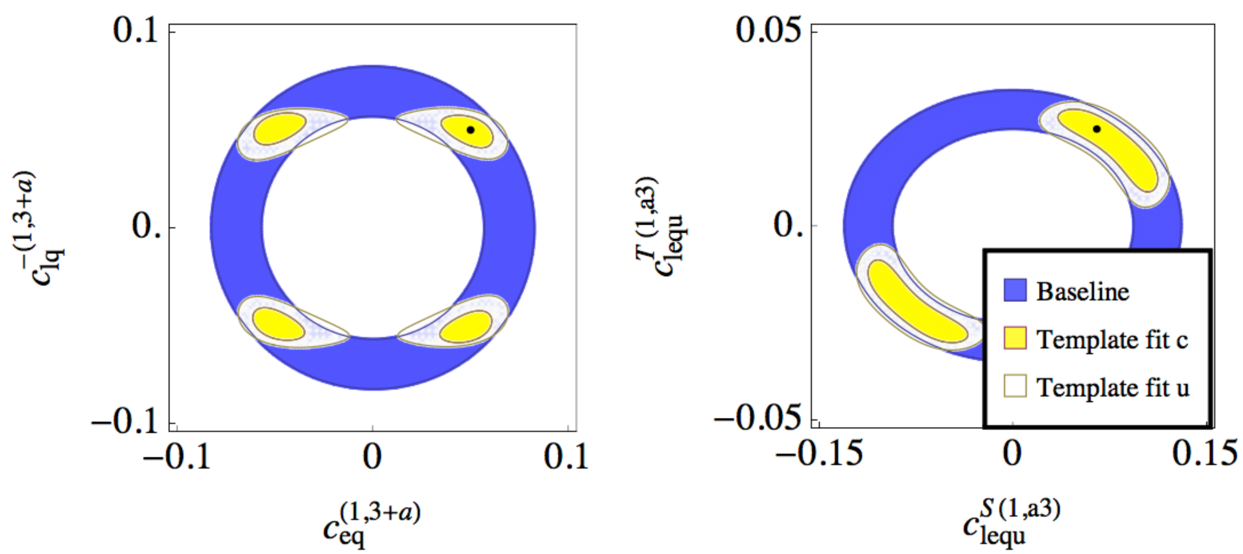

Fig. 9. Two-dimensional limits on four-fermion coefficients, at 95% CL, with other coefficients turned off. Two hypotheses are considered. Left: $c_{eq}^{(1,3+a)} = c_{lq}^{-(1,3+a)} = 0.05$. Right: $c_{lequ}^{S(1,a3)} = 0.065$, $c_{lequ}^{T(1,a3)} = 0.025$. Both points are labeled by a black dot in the plots. The template fit helps to pinpoint the coefficients. Better precision is obtained for operators involving a charm-quark (i.e. $a = 2$).

Using c-tagging

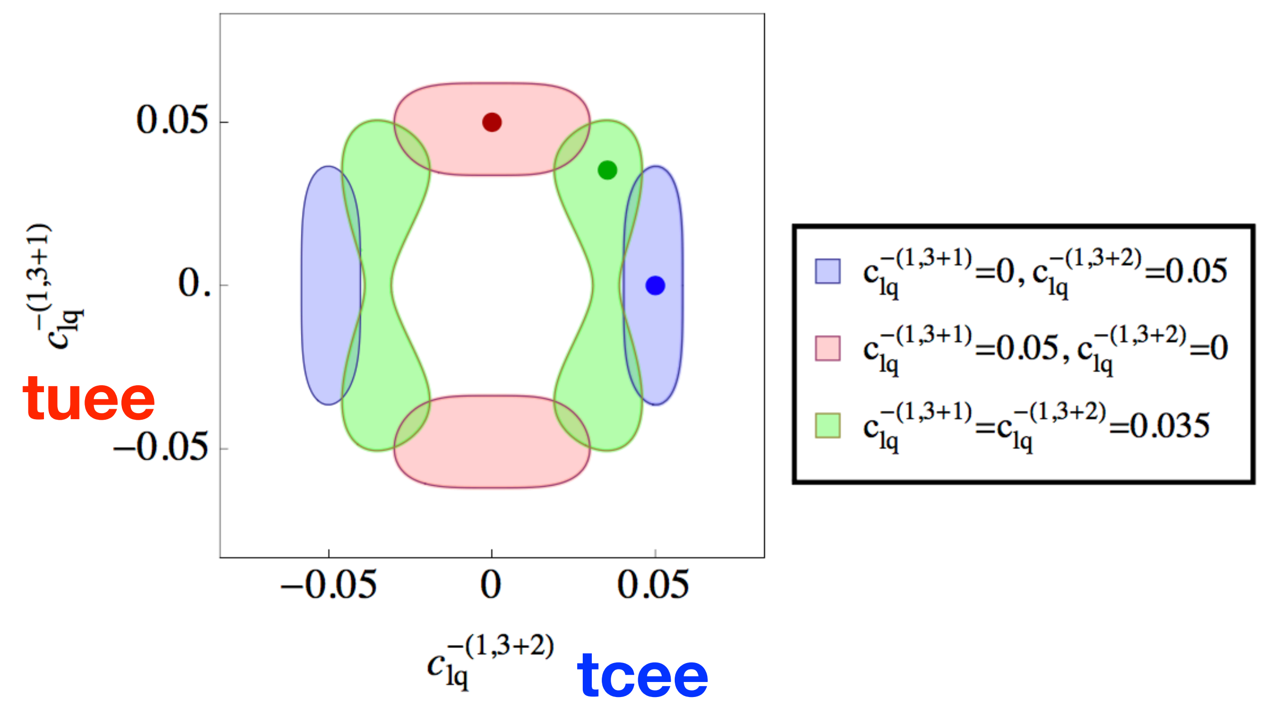

Fig. 10. Two-dimensional limits on $c_{lq}^{-(1,3+a)}$ coefficients with $a = 1$ and $a = 2$, at 95% CL. Other coefficients are turned off. Three hypotheses are considered. The template fit helps to identify the light-quark flavor involved in the FCN coupling.

In contrast to LHC:
No such info from top decay

Future plan

- Improve the simulation
  - NLO QCD for FCNC operators, consistent with LHC TOP WG. Based on [Degrande, Maltoni, Wang, CZ ’14], automated in MG. Four-fermion operators are now added.
  - ISR and beamstrahlung will be taken care of by a new MG branch (in development) by Stefano Frixione, Marco Zaro, Xiaoran Zhao
- Include other ee colliders, FCC-ee, ILC, …

With Gauthier Durieux, Benjamin Fuks, Hua-Sheng Shao, Liaoshan Shi

Conclusion

- Future ee colliders are ideal for testing top-quark flavor-changing interactions.
- In particular they have very good sensitivity on 4-fermion FCN operators, and will explore the parameter space that will be left uncovered by the HL/HE-LHC.
- Estimate for the sensitivity at CEPC 240 (as well as FCC-ee 240) looks promising. We continue to work on it, to improve the accuracy of the simulation, and to take into account more and different energies, run parameters, and different channels.

Thank you

Top FCNC: 4-fermion operators from LHC

[Chala, Santiago, Spannowsky '18]

- Recast t>qZ (->ee) at LHC is possible (though this suffers from the M_{ee} mass window cut.)
- Recast limits from LHC:

	$c_{lq}^{-(2223)}$	$c_{eq}^{(2223)}$	$c_{lu}^{(2223)}$	$c_{eu}^{(2223)}$	$c_{lequ}^{1(2223)}$	$c_{lequ}^{1(2232)}$	$c_{lequ}^{3(2223)}$	$c_{lequ}^{3(2232)}$
CR1	**8.4** (1.2)	**8.4** (1.2)	**8.4** (1.2)	**8.4** (1.2)	**18** (2.7)	**18** (2.7)	**2.3** (0.35)	**2.3** (0.35)
NEW	3.1 (1.0)	3.1 (1.0)	3.1 (1.0)	3.1 (1.0)	6.8 (2.2)	6.8 (2.2)	0.87 (0.28)	0.87 (0.28)

Table 2: Bounds on c for $\Lambda = 1$ TeV, asuming one operator at a time, using the different signal regions defined in the text. The numbers without (within) parenthesis stand for the LHC13 (HL-LHC). The boldface indicates limits using actual data. These numbers can be obtained from the master equation (2.14) using the coefficients in Table 1 and the upper bound on the following number of signal events: $s_{\max}^{CR1} = 143$ (315) and $s_{\max}^{NEW} = 18$ (179), where again the number in brackets correspond to HL-LHC projections. The projected bounds on the coefficients get a factor of ~ 3 weaker for systematic uncertainties of 10 %.

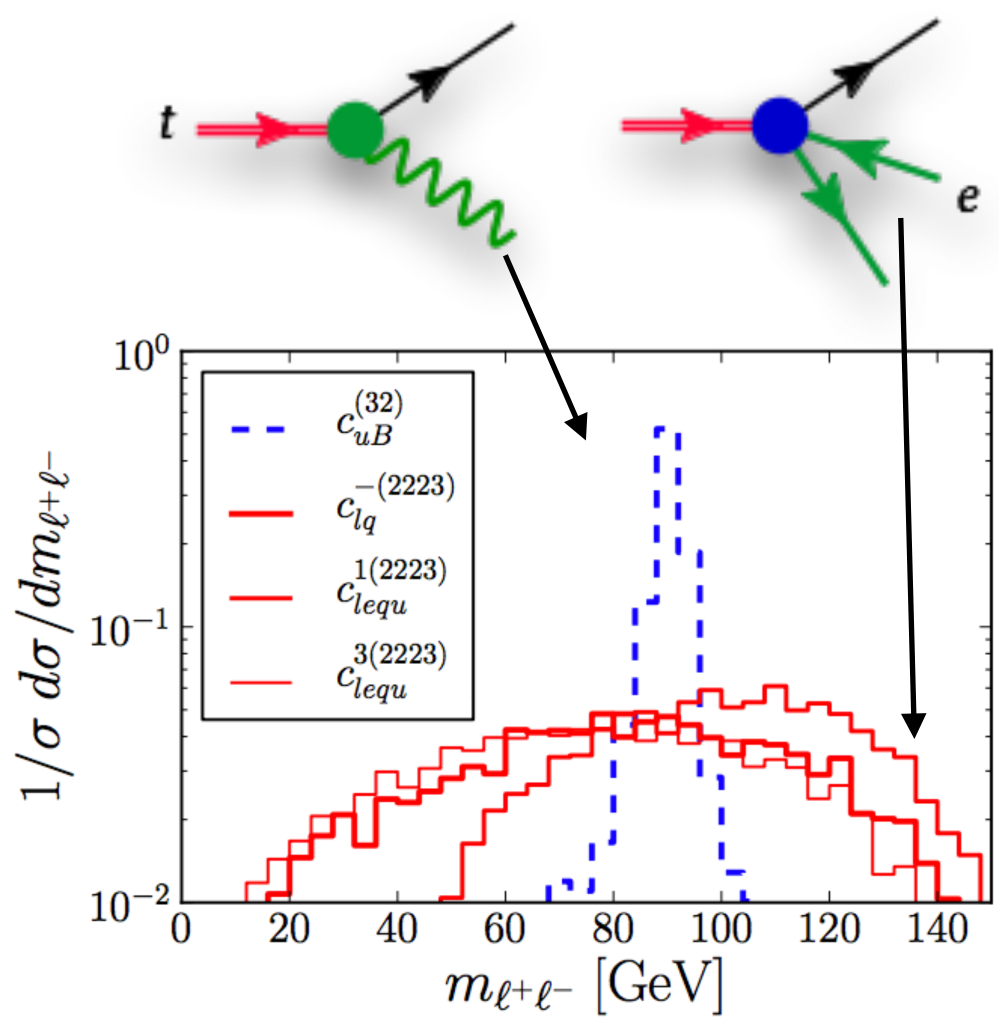

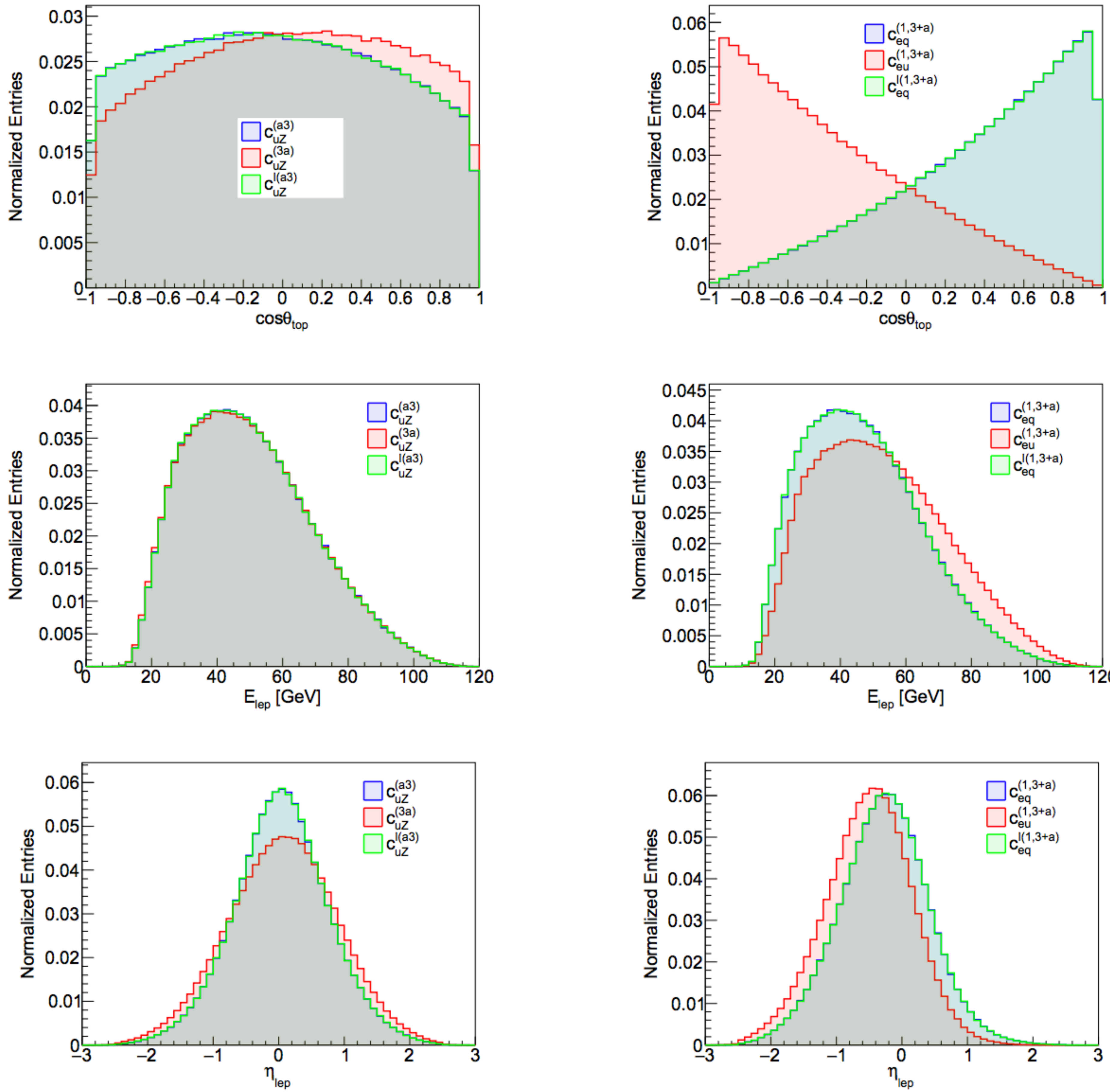
Normalized Entries
cosθtop
Elep [GeV]
ηlep
c(a3) uZ
c(3a) uZ
cl(a3) uZ
c(1,3+a) eq
c(1,3+a) eu
cl(1,3+a) eq